Received: 4 July 2024 | Revised: 8 August 2024 | Accepted: 9 August 2024

DOI: 10.1002/app.56180

RESEARCH ARTICLE

Applied Polymer SCIENCE WILEY

Crosslinked polyethyleneimine-based structures in different morphologies as promising CO_2 adsorption systems: A comprehensive study

Sahin Demirci[1] | Erk Inger[2] | Venkat Bhethanabotla[3] | Nurettin Sahiner[1,3,4]

[1]Department of Chemistry, Faculty of Science, Canakkale Onsekiz Mart University, Canakkale, Turkey

[2]Department of Airframe and Powerplant Maintenance, Atilim University, Ankara, Turkey

[3]Department of Chemical and Biomolecular Engineering, University of South Florida, Tampa, Florida, USA

[4]Department of Ophthalmology, Morsani College of Medicine, University of South Florida, Tampa, Florida, USA

Correspondence
Nurettin Sahiner, Department of Chemistry, Faculty of Science Canakkale Onsekiz Mart University, Terzioglu Campus, Canakkale 17100, Turkey.
Email: sahiner71@gmail.com

Funding information
The Scientific and Technological Research Council of Turkey, Grant/Award Number: TUBITAK-BİDEB-2219

Abstract

Although there are many studies on CO_2 adsorption via PEI-modified carbon particles, metal–organic frameworks, zeolitic imidazolate frameworks, and silica-based porous structures, only a limited number of studies on solely cross-linked PEI-based structures. Here, the CO_2 adsorption capacities of PEI-based microgels and cryogels were investigated. The effects of various parameters influencing the CO_2 adsorption capacity of PEI-based structures, for example, crosslinker types, PEI types (branched [bPEI] or linear [lPEI]), adsorbent types (microgel or cryogel), chemical-modification including their complexes were examined. NaOH-treated glycerol diglycidyl ether (GDE) crosslinked lPEI microgels exhibited higher CO_2 adsorption capacity among other microgels with 0.094 ± 0.006 mmol CO_2/g at 900 mm Hg, 25°C with 2- and 7.5-fold increase upon pentaethylenehexamine (PEHA) modification and Ba(II) metal ion complexing, respectively. The CO_2 adsorption capacity of bPEI and lPEI-based cryogels were compared and found that lPEI-GDE cryogels had higher adsorption capacity than bPEI-GDE cryogels with 0.188 ± 0.01 mmol CO_2/g at 900 mm Hg and 25°C. The reuse studies revealed that NaOH-treated GDE crosslinked bPEI and lPEI microgels and cryogels showed promising potential, for example, after 10-times repeated use >50% CO_2 adsorption capacity was retained. The results affirmed that PEI-based microgels and cryogels are encouraging materials for CO_2 capture and reuse applications.

KEYWORDS

adsorption, applications, crosslinking, oil and gas

1 | INTRODUCTION

Recent research recommended thorough strategies for diminishing and ultimately eradicating the roots for climate change, including increasing energy efficiency, utilizing renewable energy sources, reducing deforestation, planting new forests, and lowering emissions from agriculture and industry.[1–6] The Paris Agreement's goal of keeping warming to 2°C over pre-industrial levels is far from being met, and would benefit from quickly implementing strategies including renewable energy sources and forestation.[7–9] There are two often mentioned

methods for addressing this gap.[1,10] First, the methods mentioned above can be used to quicken the decarbonization process. Second, carbon dioxide emissions from smokestacks or the environment itself can be directly mitigated to counterbalance continuous emissions.

The Intergovernmental Panel on Climate Change (IPCC) has suggested that the world should use Carbon Dioxide Removal (CDR) technologies, also known as Negative Emission Technologies (NETs), to slow down global warming.[2,11] These technologies include reforestation, iron fertilization, increasing ocean alkalinity, and improving rock weathering.[12] Long-term and large-scale evidence for these claims that they might delay the peak of global CO_2 concentrations and have a better than 50% probability of keeping temperature increases below 2°C has generally not been provided.[13,14] In fact, there were several disagreements that occurred among climate scientists over whether CDR is an essential necessity or a risky diversion from reducing emissions.[1,3,4,10,12,15]

As carbon capture and storage (CCS) from industrial flue gases is categorized as an emission reduction strategy, CDR is not the same as techniques that try to stop new emissions from point sources.[12] Demand-side conservation, increased dependence on nuclear and renewable energy, supply-side efficiency improvements, and CCS technologies are some of the solutions available to reduce CO_2 emissions.[15–22] However, it is believed that fossil fuels will continue to be utilized as the main energy source in the foreseeable future because the switch to renewable energy sources is very expensive.[19,23,24] As a result, among the choices listed above, carbon capture and storage are the most sensible strategies and are the key technology for regulating the amount of CO_2 in the atmosphere.[15–21,23,24] The procedures of capturing CO_2 at the site of generation, compressing it into a supercritical fluid are essentially included in CO_2 capture and storage technology.[25–27]

For post-combustion CO_2 capture, aqueous amine solutions, such as monoethanolamine, are used for CO_2 adsorption.[19,28–30] Decades of improvement hasn't changed the technology's intrinsic constraints, which include reactor corrosion, volatile amine loss, and high regeneration energy consumption.[31–34] Solid adsorbents that are non-corrosive and can lower energy usage have emerged as viable solutions to get over these restrictions.[35–42] These days, materials with large surface areas-like silica, carbon-based particles, metal organic cages, covalent organic cages, and their amine-modified counterparts are the most often utilized materials to capture CO_2.[42–51] These materials can be made by polymerizing amine monomers inside the support pores,[52–54] grafting aminosilanes,[55–57] or impregnating polymeric amines like poly(ethyleneimine) (PEI) with amines to homogenize them in porous supports.[58–60] The two-stage zwitterion process is responsible for capturing CO_2 in the form of ammonium carbamate in the case of primary and secondary amines, according to research on the CO_2 adsorption mechanism of amine-based structures.[61,62]

Despite many studies on the CO_2 adsorption potential of PEI-modified adsorbents, there are a limited number of studies on the use of cross-linked PEI-based structures prepared from different crosslinkers. Therefore, in this study, the CO_2 adsorption potential of PEI-based microgels and cryogels were investigated as our group previously reported the potential use of PEI based materials in various application including biomedical, environment and energy.[63–68] In this comprehensive study, many factors such as the type of PEI molecule used (branched or linear), the type of crosslinker, modification and metal ion complexed forms of PEI structures were investigated, and the CO_2 adsorption capacities of PEI-based microgels and cryogels were compared. Moreover, the reuse potential of PEI-based microgels and cryogels in CO_2 adsorption studies was investigated and compared.

2 | EXPERIMENTAL

2.1 | Materials

Branched polyethyleneimine (bPEI, 50% in water, Mn: 1800, Sigma Aldrich), and linear polyethyleneimine (lPEI) were used as precursors in the synthesis PEI based microgels and cryogels. Poly(2-ethyl-2-oxazoline) (PEOX, Mn: 50000, PDI 3-4, Sigma Aldrich, USA), hydrochloric acid (HCl, 37%, Carlo Erba, France), and sodium hydroxide (NaOH, 99%, AFG Bioscience, USA) were used for the preparation of linear polyethyleneimine (lPEI). Dioctyl sulfosuccinate sodium salt (AOT, 98%, Sigma Aldrich), and l-alpha-lecithin (granular, 98%, Acros) were used as surfactants, and gasoline (Total, 98 octane, local vender in Turkey) was used as a solvent, divinyl sulfone (DVS, 98%, Merck), glycerol diglycidyl ether (GDE, ≤100%, Sigma Aldrich), and phosphonitrilic chloride (PNC, 99%, Sigma Aldrich) were used as crosslinkers to synthesis PEI based microgels. GDE crosslinker was also used as crosslinker to prepare PEI based cryogels. The 2-bromoethylamine hydrobromide (BrEtA, 99%, Aldrich), pentaethylenehexamine (PEHA, 96%, Sigma Aldrich), epichlorohydrin (ECH, 99%, Sigma Aldrich), and dimethylformamide (DMF, 99%, Carlo Erba) were used for modification reactions. Calcium chloride (99%, Carlo Erba), Magnesium nitrate (99%, Sigma Aldrich), and Barium chloride (99%, Merck) salts were used as metal ion sources. Sodium hydroxide (NaOH, 99%, AFG Bioscience) was used for deprotonation of PEI based

structures. Double distilled water, ethanol (99% Carlo Erba), and acetone (99%, Sigma Aldrich) were used as mediums for washing processes.

2.2 | Synthesis of materials

2.2.1 | Crosslinked PEI-based microgels

Microgel synthesis

The synthesis of PEI-based microgels was carried out by using various chemicals as crosslinker by following literature with some modifications.[64–66] To synthesis bPEI-based DVS and PNC crosslinked microgels, 1 mL of bPEI solution (50% in water, Mn:1800 g/mol) was placed into 30 mL 0.1 M AOT/gasoline solution. After adding 100% DVS and PNC %mole based on the repeating unit of bPEI, they were mixed at room temperature for 2 h for cross-linking reactions. Subsequently, the respective mixtures were precipitated by transferring them into excess acetone and washed as in the reported studies.[64,66]

For the synthesis of GDE cross-linked bPEI microgels, 1 mL of 50% aqueous bPEI solution was added to 30 mL of lecithin/gasoline medium and the prepared solution was placed in an oil bath set at 50°C and mixed at a stirring speed of 1000 rpm. After the solution was mixed in a 50°C oil bath for 20 min, GDE crosslinker (100% mol based on the PEI molecule) was added and stirred for 4 h at a stirring rate of 1000 rpm. Also, the GDE crosslinked lPEI microgels were synthesized as mentioned above. Briefly, 0.2 of lPEI was dissolved in 1 mL water at 80°C and transferred to 30 mL of lecithin solution prepared in gasoline and placed in an oil bath at 50°C, and the crosslinker, GDE (100% mol based on the molecule of lPEI) was added quickly and mixed for another 4 h at a stirring rate of 1000 rpm. Subsequently, the prepared GDE crosslinked bPEI and lPEI microgels were washed as in the reported studies.[65]

The prepared DVS, PNC, and GDE crosslinked bPEI microgels were called bPEI-DVS, bPEI-PNC, and bPEI-GDE microgels, respectively. The prepared GDE crosslinked lPEI microgels were also called lPEI-GDE microgels.

All the prepared PEI-based microgels were treated with NaOH to deprotonate the amine groups on the microgels. For the deprotonation process, a certain amount of PEI-based microgels (1 g) was placed in 100 mL 1 M NaOH solution and mixed for 2 h at a stirring speed of 250 rpm. After NaOH treatment, PEI-based microgels were washed three times with pure water to remove excess NaOH from the structure, then washed once with acetone and dried with a heat gun. After that, the NaOH treated all PEI-based microgels that were stored in closed tubes for further usage.

Cryogel synthesis

A few minor adjustments were made to the procedure documented in the literature in order to prepare the bPEI cryogels.[67] Consequently, a vial containing 7.5 mL of water and 1 mL of bPEI (50% aqueous solution) was filled. Following a 1-min cooling period at −20°C in a deep freezer, 400 μL of GDE was added, and the liquid was quickly vortexed for 1 min before being placed into plastic pipettes measuring eight millimeters in diameter. The plastic pipettes were then immediately put in a deep freezer that was set to −20°C for a 24-h cryo-gelation/cryo-crosslinking process.

The preparation of lPEI cryogels were also done via following reported study in literature by our group.[68] The preparation of lPEI from PEOX was carried out by following literature.[68,69] To summarize, the prepared lPEI mixture in 10 mL of 0.25 M NaOH at a concentration of 0.1 g/mL was dissolved at 80°C. After seeing the clear lPEI solution, 0.237 mL of GDE (5% mol ratio relative to the lPEI repeating unit (—CH_2CH_2NH—, 43 g/mol)) was added to the reaction medium. It was then vortexed for 30 s and immediately put on plastic pipettes with a 7 mm diameter. After that, plastic pipettes were immediately placed into a freezer at −20°C and kept there for 24 h to complete cryo-gelation/cryo-crosslinking reactions.

The prepared bPEI and lPEI cryogels were cut in similar shape and sizes (cylindrical, 0.5 × 0.7 cm) and washed with water several times to remove unreacted reagents. The PEI-based cryogels were also treated with NaOH as mentioned above to deprotonate amine groups.

2.3 | Characterization

The scanning electron microscopy (SEM, GAIA3, Tescan, and Jeol JSM-5600) images of PEI and lPEI based microgels were obtained after coating the samples on SEM stubs to few nanometer-sized Pd with a working voltage of 20.0 kV.

Fourier Transform Infrared Radiation (FT-IR, iS10, ThermoScientific) spectroscopy was used to identify the functional groups of bPEI, and lPEI-based microgels and cryogels. FT-IR spectra were acquired by recording 16 consecutive scanning sweeps of spectra in the 4000–650 cm^{-1} range using the ATR method.

By a thermogravimetric analyzer (TGA, SII TG/DTA6300, Exstar), the thermal degradation profile of cryogels and microgels based on bPEI and lPEI were investigated. In TGA analysis, 3–5 mg of sample were placed in TGA pan and heated to 100°C to remove

the moisture. Following that, the temperature was raised to 750°C from 100°C at a rate of 10°C/min at a 20 mL/min N_2 gas flow, and the sample's weight changes with temperature were noted.

The ZetaPals analyzer system (90 Plus, BIC, and Nanobrook Omni, Brookhaven) were used to assess the zeta potential of bPEI and lPEI based microgels. The samples were suspended in 40 mL of 1 mM KCl (for 90 Plus) and KNO_3 (for Nanobrook) at a concentration of 1 mg/mL.

The surface areas, pore volume, and pore size of microgels based on bPEI and lPEI were analyzed using the Brunauer–Emmett–Teller (BET) technique. This analysis was conducted using a N_2 adsorption/desorption apparatus (Micromeritics, Tristar II Surface and Porosity). Before analysis, samples subjected to degassing using a Flow Prep 060 degasser to eliminate moisture and impurities at a temperature of 100°C for a duration of 12 h.

The porosity% values of bPEI-GDE and lPEI-GDE cryogels were also calculated according to Equation (1);

$$\text{Porosity}\% = (m_s - m_d)/m_s \text{ x } 100 \quad (1)$$

where, "m_s" names the weight of the water-swollen cryogels, "m_d" is the weight of washed and freeze-dried cryogel samples, respectively.

2.4 | The modification of GDE crosslinked bPEI and lPEI microgels

Bromo ethylamine (BrEtA) and pentaethylenehexamine (PEHA) were used as modification agents for the modification of PEI-based microgels. The modification process was carried out by following the studies reported by our group in the literature.[70,71] Accordingly, for the modification of PEI-based microgels with BrEtA, a certain amount (0.5 g) of PEI-based microgels was added to 100 mL of ethanol, in which BrEtA was dissolved according to the repeating units of the structures (1.5-fold) and mixed for 12 h at a stirring speed of 250 rpm. Then, BrEtA-modified PEI-based microgels were washed twice with ethanol to remove unreacted BrEtA and dried. Thereafter, the dried BrEtA-modified PEI-based microgels were deprotonated by treatment with 100 mL 1 M NaOH and washed with pure water three times, then dried and stored in closed containers for further use.

For the modification of PEI-based microgels with PEHA, the relevant microgels were added to 50 mL of dimethylformamide (DMF) and after adding two times the amount of microgel by weight of epichlorohydrin (EPC), they were mixed at a mixing speed of 500 rpm in a mixer set at 90°C for 1 h. Then, it was taken from the reaction medium, washed twice with DMF and added into 50 mL of DMF again, then PEHA was added equal to the mole of EPC added to the medium and the reaction was stirred for another 1 h at 90°C. At the end of the reaction, the prepared PEHA modified PEI-based microgels were washed twice with DMF and twice with acetone and then dried.

Finally, the prepared BrEtA and PEHA modified PEI-based microgels were deprotonated by treatment with 100 mL 1 M NaOH and washed with pure water twice, then dried and stored in closed containers for next use.

2.5 | Preparation of metal ion complexes of GDE crosslinked bPEI and lPEI microgels

Here, Ca(II), Mg(II) and Ba(II) ions were loaded onto NaOH treated PEI-based microgels by adsorption method. Accordingly, NaOH treated PEI-based microgels were placed in 100 mL aqueous Ca(II), Mg(II) and Ba(II) metal ion solutions prepared at 1000 ppm concentrations and mixed at a stirring speed of 500 rpm at room temperature for 6 h. Then, NaOH treated PEI-based microgel complexes with metal ion adsorption were washed once with pure water to remove the metal ions attached to the surface, and after drying, they were stored in closed containers for further use.

2.6 | CO_2 adsorption studies via PEI-based microgels and cryogels

CO_2 adsorption capacities of PEI-based microgels and cryogels were determined with a surface area and porosity device connected to a CO_2 (99.9%) gas tube at 900 mm Hg pressure and 25°C temperature. For this purpose, before CO_2 adsorption studies, washed and dried PEI-based microgels and cryogels were degassed under N_2 (99.9%) gas at 80°C for 12 h.

However, for the reuse of PEI-based microgels and cryogels in the CO_2 adsorption process, the CO_2 adsorbed structures were kept at 120°C for 6 h to desorb adsorbed CO_2, and the reuse potential of the prepared systems was determined by examining their CO_2 adsorption capacities after degassing under N_2 gas at 80°C for 12 h.

3 | RESULTS AND DISCUSSION

3.1 | The synthesis and characterization of PEI-based microgels and cryogels

In our previous studies, the preparation and characterization of DVS, GDE, and PNC crosslinked bPEI microgels

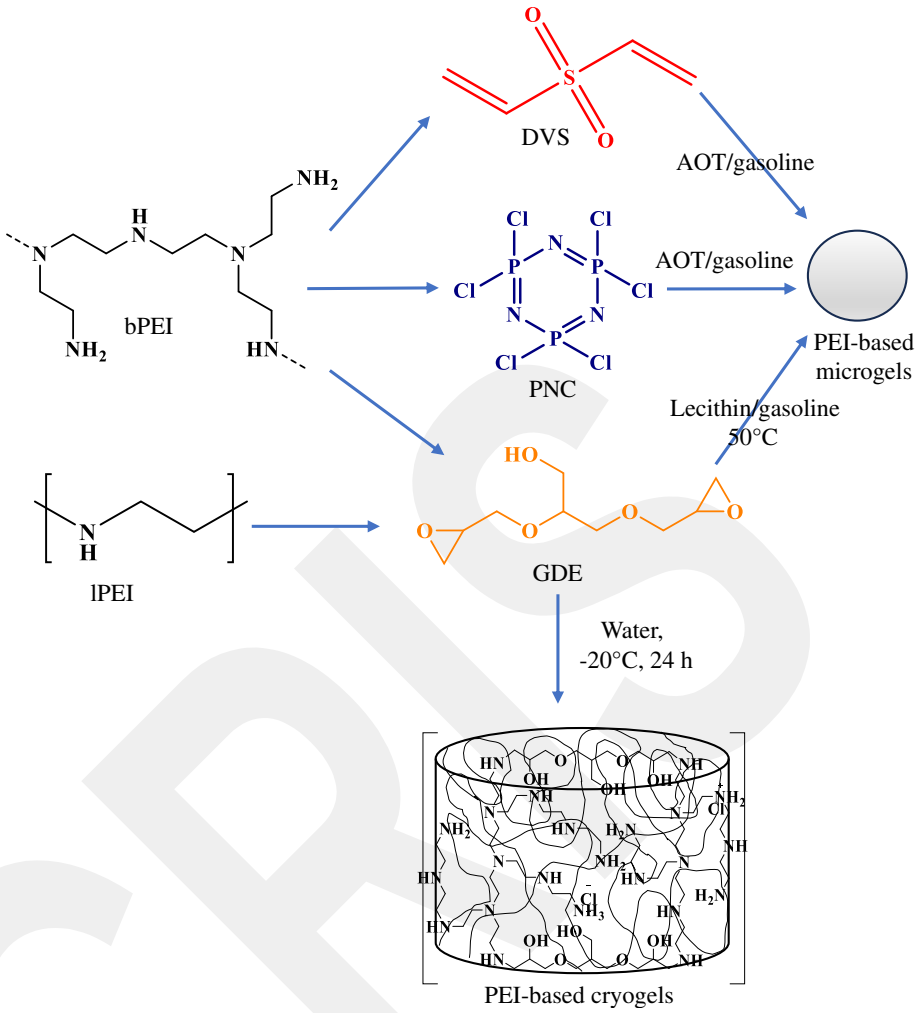

FIGURE 1 The chemical structure of bPEI, lPEI, and crosslinkers are used for synthesis bPEI- and lPEI-based microgels and cryogels. [Color figure can be viewed at wileyonlinelibrary.com]

were described in detail.[64–66] The chemical structures of bPEI, DVS, PNC, and GDE are given in Figure 1. Different crosslinkers that can be used to prepare bPEI-based microgels also affords some kind of heteroatom doping into the structures. For example, the crosslinking reaction between DVS and bPEI occurred via Michael addition reactions,[64] and this DVS crosslinked bPEI microgels contain sulfur atoms coming from DVS. On the other hand, the bPEI-PNC microgels prepared via the reactions between PNC and amine groups of PEI,[66] and PNC crosslinked bPEI microgels contain phosphorous atoms coming from PNC. Moreover, the ring opening reactions[65] between GDE and bPEI used for bPEI-GDE microgels preparation render oxygen atoms into the structure. Since the cross-linking reactions took place in a reverse-micelle microemulsion medium, the prepared bPEI-based microgels attained are spherical in shape. The size ranges of bPEI-DVS microgels were found in 0.5–10 μm range from the SEM analysis.[64] Similarly, the sizes range of spherical bPEI-PNC microgels were reported in 5–30 μm.[66] On the other hand, bPEI-GDE microgels exhibits broad size distribution varying from 20 to 200 μm.[65] The differences between sizes of bPEI-DVS/bPEI-PNC microgels and bPEI-GDE microgels can be explained with the effect of used surfactants, AOT and lecithin and the nature and the extent of the crosslinkers.

Moreover, the successful synthesis of all bPEI-DVS, bPEI-PNC, and bPEI-GDE microgels were confirmed via FT-IR spectrums.[64–66] The peaks observed at about 1030, 1120, and 1363 cm^{-1} are attributed to S═O stretching, SO_2 symmetric stretching, and asymmetric stretching confirming the formation of bPEI-DVS microgels.[64] The successful synthesis of bPEI-PNC microgels was also established via the observed peak at 1167 cm^{-1} which is assigned to P═N vibrations.[66] On the other hand, the detected ether peak at about 1113 cm^{-1} for bPEI-GDE microgels from the FT-IR spectra confirmed the relevant crosslinking reaction.[65] The thermal stability of microgels bPEI-DVS, bPEI-PNC, and bPEI-GDE microgels were compared[64–66] and determined that bPEI-PNC microgels is thermally more stable with almost no weight lost up to 300°C,[66] whereas the bPEI-DVS started to degrade at about 200°C,[64] and bPEI-GDE microgels started to degrade around 150°C.[65] Also, the determined zeta

potential values of bPEI-DVS, and bPEI-PNC microgels were reported as +12.3 ± 1.2 mV and + 18.6 ± 1.1 mV, respectively, from their corresponding solutions in 1 mM KCl at 1 mg/mL concentrations.[63,66]

The zeta potential values of bPEI-GDE microgels were measured as +9.1 ± 1.1 mV from its 1 mg/mL solution in 1 mM KNO_3. SEM images, FT-IR spectrum, and TGA thermogram of prepared lPEI-GDE microgels were also given in Figure S1. It was clearly seen from the SEM images in Figure S1, the lPEI-GDE microgels are in spherical shape with size range between 0.2–5 μm scales. The comparisons of the FT-IR spectrum of lPEI-GDE microgels and lPEI are given in Figure S1, the most distinct differences were observed for the —OH bending peaks at 1391 cm^{-1}, and ether peaks at 1113 and 1071 cm^{-1} due to the GDE crosslinking, however, the characteristic peaks of lPEI as N—H stretching at 3286 cm^{-1}, C—H stretching at 2982 and 2856 cm^{-1}, N—H bending at 1653 cm^{-1}, and C—N stretching at 1066 cm^{-1} were observed for both lPEI and lPEI-GDE microgels. The TGA thermograms given in Figure S1 showed that lPEI chains started degrading at about 140°C, whereas the lPEI-GDE microgels were found thermally stable up to 180°C without weight loss. The lPEI started to degrade between 150 and 190°C with 13% weight loss and continued to degrade 54% by weight in the 240–330°C range, and 92% cumulative weight loss in 340–590°C. On the other hand, the lPEI-GDE microgels started to degrade firstly the in 180–320°C range with 48 wt%, and the second degradation step was observed in the 410–440°C range with 84% cumulative weight loss. The zeta potential value for lPEI-GDE microgels was measured as +6.9 ± 1.3 mV at 1 mg/mL concentration from its solution in 1 mM KNO_3.

The surface area, pore volume, and pore size values for prepared bPEI, and lPEI-based microgels were also investigated via N_2 adsorption/desorption measurements. However, no results were obtained for bPEI-DVS, bPEI-GDE, and lPEI-GDE microgels, and these materials were assumed as nonporous structures. On the other hand, the surface area, pore volume, and pore size values for bPEI-PNC microgels were measured as 50.9 m^2/g, 0.33 cm^3/g, and 25.2 nm, respectively.[66]

Detailed characterization of prepared bPEI-GDE and lPEI-GDE cryogels were also carried out at our previously reported studies in literature,[68,72] and schematic presentation is given in Figure 1. In brief, the synthesis of bPEI-GDE and lPEI-GDE cryogels were carried out under cryogenic conditions (below melting point of solvent which is water in here). The bPEI and lPEI cryogels prepared by cryo-crosslinking reaction, below the solvent's freezing point (water), the ice crystals formed were utilized as pore-forming agents. Water is used as a solvent while PEI and the crosslinker are used as the precursors, the ice crystals form upon cooling and the concentrations of the precursors around produced ice crystals were increased allowing the crossing reaction between the precursors readily. Upon completion of reaction (24 h), the ice crystals thawed at room temperature leading to interconnected super porous cryogel network structures. The interconnected super porous structures of bPEI-GDE and lPEI-GDE cryogels were reported earlier clearly in SEM images.[68,72] It was observed that, the pore size ranges of PEI based cryogels were between 1 and 200 μm.[68,72] The porosity% values for bPEI-GDE and lPEI-GDE cryogels were determined as 78 ± 5,[72] and 63 ± 5,[68] respectively. The successful synthesis of related cryogels were confirmed with FT-IR spectrum, and TGA thermograms showed that PEI based cryogels were thermally stable up to 250°C.[68,72]

The CO_2 adsorption of solid materials containing amines has been explained by two different processes.[73] Therefore, the suggested processes are, respectively, an acid–base reaction in which tertiary amines react with CO_2 in the presence of water to generate bicarbonate or primary and secondary amines react with CO_2 via a zwitterion mechanism to form a carbamate.[62,74] Deprotonation of amine groups is required in the zwitterion pathway to generate a carbamate. When adsorption occurs in a wet environment, a nearby amine group or hydroxyl ion can readily provide this need. It was found that primary amines had much better adsorption capabilities than secondary and tertiary amines when the adsorption characteristics of various amine structures for CO_2 capture were investigated.[61,73,75,76] Therefore, the potential CO_2 adsorption application of PEI-based microgels and cryogels reported by our group were investigated. Thus, the CO_2 adsorption capacities of bPEI microgels prepared with different crosslinkers containing different heteroatoms were explored. In addition, the effects of branched or linear polymer and the types of amines, for example, primary, secondary, tertiary in PEI structure on CO_2 adsorption were investigated by comparing the CO_2 adsorption capacities of the microgels prepared from both branched and linear PEI chains. Moreover, a comparison was made by examining the CO_2 adsorption abilities of crosslinked PEI-based structures, for example, with spherical or superporous morphologies.

3.2 | CO_2 adsorption capacities of PEI-based microgels

The potential CO_2 adsorption capacities of prepared PEI-based microgels were given in Figure 2a–c. The

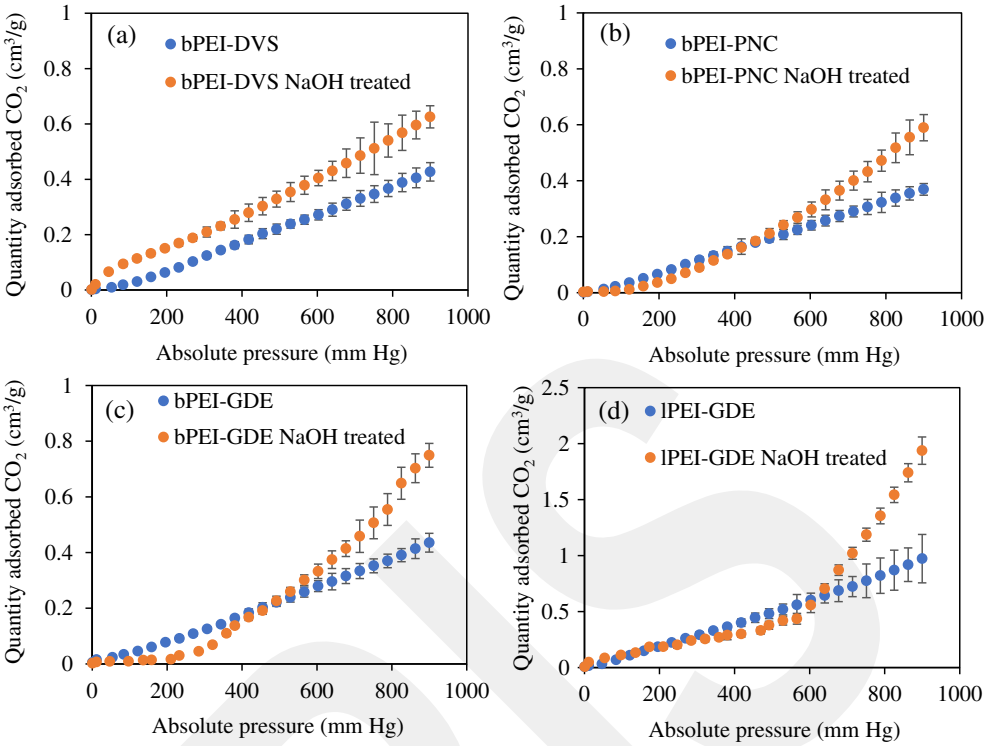

FIGURE 2 The comparison of CO_2 adsorption ability of bare, and NaOH treated (a) bPEI-DVS (b) bPEI-PNC, (c) bPEI-GDE, and (d) lPEI-GDE microgels. [Color figure can be viewed at wileyonlinelibrary.com]

adsorption capacities of PEI-DVS, PEI-PNC, PEI-GDE microgels, and their related NaOH treated forms were compared. In Figure 2a, it was clearly seen that the adsorbed CO_2 amount linearly increased with the increasing pressure up to 900 mm Hg at 25°C. The bPEI-DVS microgels adsorbed 0.43 ± 0.03 cm^3 CO_2/g at 900 mm Hg and 25°C, whereas almost 1.5-fold higher CO_2 adsorption was observed for NaOH treated bPEI-DVS microgels at same pressure and temperature with 0.62 ± 0.04 cm^3 CO_2/g. On the other hand, in Figure 2b, the CO_2 adsorption capacity of bPEI-PNC and NaOH treated bPEI-PNC microgels at 900 mm Hg and 25°C were determined as 0.37 ± 0.02 and 0.59 ± 0.05 cm^3 CO_2/g, respectively.

Moreover, the comparison of CO_2 adsorption capacities of bPEI-GDE and NaOH treated bPEI-GDE microgels were also given in Figure 2c. The CO_2 adsorption capacity of bPEI-GDE microgels were determined as 0.44 ± 0.03 cm^3 CO_2/g at 900 mm Hg and 25°C. On the other hand, the CO_2 adsorption by NaOH treated bPEI-GDE microgels was observed as less than bPEI-GDE microgels up to 400 mm Hg, however exhibited higher CO_2 adsorption capacity than bPEI-GDE microgels at 900 mm Hg and 25°C with 0.75 ± 0.04 cm^3 CO_2/g. In addition, the CO_2 adsorption capacity of lPEI-GDE microgels and its NaOH treated form were also compared in Figure 2d. A similar tendency with NaOH treated bPEI-GDE microgels was also observed for NaOH treated lPEI-GDE microgels as less amount of CO_2 adsorption up to almost 600 mm Hg at 25°C. However, the lPEI-GDE microgels exhibited 0.97 ± 0.22 cm^3 CO_2/g adsorption, which increased to 1.93 ± 0.12 cm^3 CO_2/g at 900 mm Hg and 25°C after NaOH treatment.

TABLE 1 The comparison of CO_2 adsorption capacities of PEI based microgels done at 25°C temperature and 900 mmHg pressures.

Materials (microgels)	Quantity adsorbed CO_2 (mmol/g)
bPEI-DVS	0.021
bPEI-DVS NaOH	0.030
bPEI-PNC	0.018
bPEI-PNC NaOH	0.028
bPEI-GDE	0.021
bPEI-GDE NaOH	0.036
bPEI-GDE BrEtA	0.019
bPEI-GDE BrEtA NaOH	0.044
bPEI-GDE PEHA	0.025
bPEI-GDE PEHA NaOH	0.067
lPEI-GDE	0.047
lPEI-GDE NaOH	0.094
lPEI-GDE BrEtA	0.039
lPEI-GDE BrEtA NaOH	0.104
lPEI-GDE PEHA	0.049
lPEI-GDE PEHA NaOH	0.119

The adsorbed amount of CO_2 by PEI-base microgels in millimole CO_2 unit at 900 mm Hg and 25°C were summarized in Table 1 to clear comparison of adsorption capacities. According to results, the bPEI-DVS, and bPEI-PNC microgels adsorbed 0.021 ± 0.002 and 0.018 ± 0.001 mmol CO_2/g, respectively. On the other hand, the adsorbed amount of CO_2 by bPEI-GDE, and lPEI-GDE microgels were calculated as 0.021 ± 0.002 and 0.047 ± 0.01 mmol CO_2/g, respectively.

On the other hand, the NaOH treatment of related microgels increased the adsorbed amount of CO_2. The CO_2 adsorption with NaOH treated bPEI-DVS, bPEI-PNC, bPEI-GDE, and lPEI-GDE microgels were calculated as 0.030 ± 0.002, 0.028 ± 0.002, 0.036 ± 0.002, and 0.094 ± 0.006 mmol CO_2/g, respectively. In overall, the adsorbed amounts of CO_2 by bPEI-DVS and bPEI-GDE are more than bPEI-PNC microgels. Moreover, the higher CO_2 adsorption capacity was observed for NaOH treated bPEI-GDE microgels among the NaOH treated bPEI-based microgels. On the other hand, among all PEI-based and NaOH treated PEI-based microgels the higher CO_2 adsorption was observed for NaOH treated lPEI-GDE microgels with at least 2.5-fold higher CO_2 adsorption. The increase in CO_2 adsorption capacity for PEI based microgels upon NaOH treatment can be explained through deprotonation of amine groups on PEI structure,[65] which is the zwitterionic structure, developed by CO_2 adsorption.[62,75] The schematic presentation of the effect of deprotonation of PEI-based microgels on CO_2 adsorption capacity according to zwitterion mechanism (Equation 2) are illustrated in Figure S2.

$$R\text{-}NH_2 + CO_2 \rightarrow R\text{-}^{+}NH_2\text{-}^{-}CO_2 \quad (2)$$

The bare PEI based microgels contain protonated amine groups on their structure naturally, as was confirmed with positive zeta potential values. The naturally protonated amine groups on PEI-based microgels structure prevent CO_2 bonding from those sides. On the other hand, the deprotonation of amine groups with simple aqueous NaOH treatment affords bonding ability to amine groups on structure. On the other hand, the higher CO_2 adsorption observed for lPEI based microgels can be explained with oxidation rates of amine groups. It is well known that isolated primary amines are more stable than isolated secondary amines.[57,77] When it comes to PEI, the branching PEI with a combination of primary, secondary, and tertiary amines is less stable than the linear PEI, which primarily contains secondary amines.[78] It was suggested that the oxidative breakdown of amines can be impacted by the coexistence of several amine types.[78,79]

3.2.1 | Effect of modification on CO_2 adsorption capacity of GDE crosslinked PEI-based microgels

As a result of the studies, it was understood that bPEI and lPEI microgels crosslinked with GDE had the highest CO_2 adsorption capacity. For this reason, GDE crosslinked bPEI and lPEI microgels were modified with BrEtA and PEHA, which contain different numbers of amine groups in their structures, and the changes in their CO_2 adsorption capacities were examined. The schematic representation of modification reactions of PEI based microgels are given in Figure S3. Here, BrEtA reacts with the amine groups of PEI-based microgels from its bromine sides and introduces extra amine groups into the structure.[70] On the other hand, in PEHA modification, EPC, which is used as an intermediate agent, binds to PEI-based microgels from the epoxy side with ring-opening reactions and reacts with PEHA from the exposed chlorine side, providing at least one primary and five secondary amines to the structure.[71] It was thought that the CO_2 adsorption capacity of PEI-based microgels prepared here could increase. In Figure 3a, the adsorption capacities of BrEtA modified bPEI-GDE was determined as 0.38 ± 0.03 cm^3 CO_2/g, which is a little lower than bare bPEI-GDE microgels, however after NaOH treatment of BrEtA modified bPEI-GDE the CO_2 adsorption capacity increased to 0.90 ± 0.09 cm^3 CO_2/g at 900 mm Hg and 25°C. Similarly, in Figure 3b, the CO_2 adsorption capacity of lPEI-GDE microgels slightly decreased to 0.81 ± 0.08 cm^3 CO_2/g after BrEtA modification and increased to 2.16 ± 0.17 cm^3 CO_2/g at 900 mm Hg and 25°C after NaOH treatment of BrEtA modified lPEI-GDE microgels.

On the other hand, the CO_2 adsorption capacities of PEHA modified bPEI and lPEI based GDE crosslinked microgels were also compared in Figure 3c,d, respectively. The CO_2 adsorption with PEHA modified bPEI-GDE microgels was observed as 0.51 ± 0.04 cm^3 CO_2/g at 900 mm Hg and 25°C, which is slightly higher than bare bPEI-GDE microgels and increased to 1.39 ± 0.15 cm^3 CO_2/g for NaOH treated PEHA modified bPEI-GDE microgels under same conditions. Moreover, the CO_2 adsorption capacities of PEHA modified lPEI-GDE and NaOH treated lPEI-GDE microgels were determined as 1.01 ± 0.11 and 2.48 ± 0.28 cm^3 CO_2/g, respectively, which are higher than CO_2 adsorption capacity of bare lPEI-GDE microgels.

The effect of modification on CO_2 adsorption capacities of PEI-base microgels in mmol CO_2 unit at 900 mm Hg and 25°C were summarized in Table 1 to clear comparison. It was observed that the BrEtA modified bPEI-GDE, and lPEI-GDE microgels adsorbed 0.019 ± 0.001

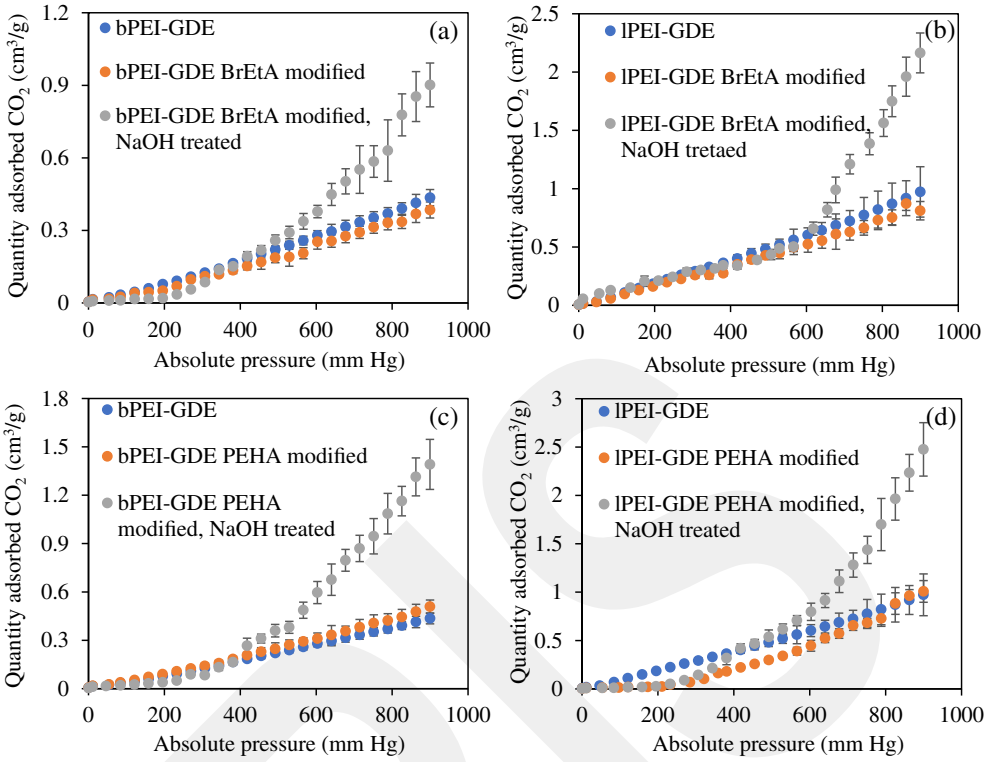

FIGURE 3 The comparison of CO_2 adsorption ability of bare, and NaOH treated form of BrEtA modified (a) bPEI-GDE (b) lPEI-GDE microgels, and PEHA modified (c) bPEI-GDE, (d) lPEI-GDE microgels. [Color figure can be viewed at wileyonlinelibrary.com]

and 0.039 ± 0.004 mmol CO_2/g, respectively, which are increased to 0.044 ± 0.004 and 0.10 ± 0.008 mmol CO_2/g after NaOH treatment of related microgels. Moreover, the CO_2 adsorption amount for PEHA modified bPEI-GDE, and lPEI-GDE microgels were calculated as 0.025 ± 0.002 and 0.049 ± 0.005 mmol CO_2/g, respectively. The adsorbed amount of CO_2 by NaOH treated PEHA modified bPEI-GDE, and lPEI-GDE microgels increased to 0.067 ± 0.007 and 0.12 ± 0.01 mmol CO_2/g, respectively. According to the modification reactions shown in Figure S3, HBr is released as a by-product during BrEtA modification, and HCl is released as a by-product during PEHA modification. These HBr and HCl released as a result of the reaction react with other amine groups in the structure and cause the protonation of the structure,[70,71] and it could explain the decreasing on CO_2 adsorption capacities of PEI-based microgels after modification. Also, at least 2-fold increasing on adsorbed amount of CO_2 after NaOH treatment of modified PEI-based microgels can be explained with the increasing of number of deprotonated amine groups on structures.

3.2.2 | Effect of metal ions on CO_2 adsorption capacity of GDE crosslinked PEI-based microgels

In recent years metal ion doping of materials has been suggested to improve gas adsorption capacities.[80–85]

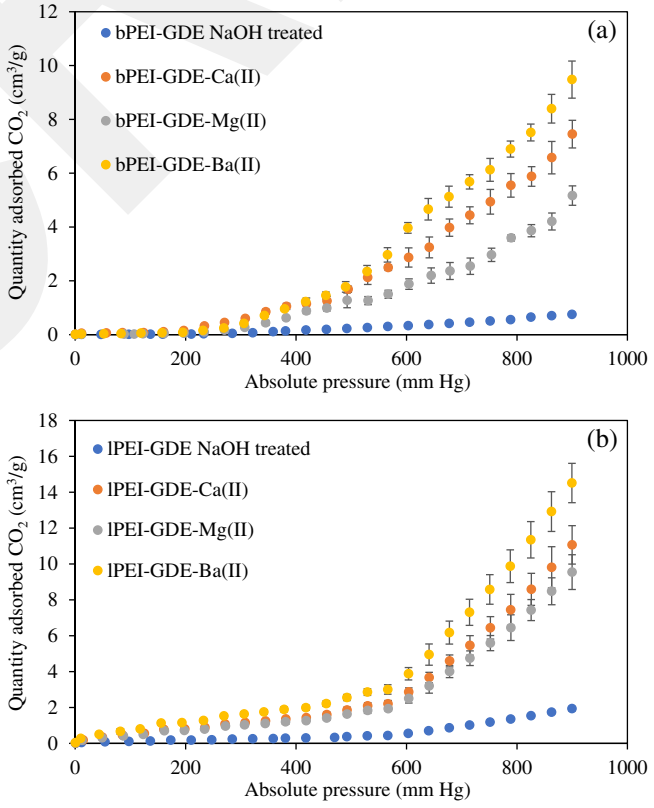

FIGURE 4 The comparison of CO_2 adsorption ability of (a) NaOH treated form bPEI-GDE, and (b) lPEI-GDE microgels with corresponding Ca(II), Mg(II), and Ba(II) metal ions adsorbed forms. [Color figure can be viewed at wileyonlinelibrary.com]

TABLE 2 The comparison of CO_2 adsorption capacities of PEI-M(II) (M: Ca(II), Mg(II), and Ba(II)) microgel complexes done at 25°C temperature and 900 mmHg pressures.

Materials (microgels)	Quantity adsorbed CO_2 (mmol/g)	Fold increase
bPEI-GDE NaOH	0.036	-
bPEI-GDE Ca(II)	0.36	~10
bPEI-GDE Mg(II)	0.25	~7
bPEI-GDE Ba(II)	0.46	~13
lPEI-GDE NaOH	0.094	-
lPEI-GDE Ca(II)	0.53	~6
lPEI-GDE Mg(II)	0.46	~5
lPEI-GDE Ba(II)	0.70	~7.5

According to the literature review, potassium tethering with a carbon matrix can boost the flue gas mixture's ability to capture CO_2.[86] CO_2 is more evenly absorbed by calcium embedding on the C2N structure than by other transition metals including Sc, Ti, V, Cr, Mn, Fe, and Co.[87] To increase the CO_2 adsorption capacity of MOFs,[88] phosphorene,[83] lithium silicate,[89] and so forth, lithium-ion doping has been applied widely. In the literature, ion-doped materials with Li^+, Na^+, K^+, Cs^+, Ca^{2+}, Mg^{2+}, and Ba^{2+} were also investigated for CO_2 adsorption.[84,90–92] In here, the changing on adsorption capacities of NaOH treated bPEI-GDE, and lPEI-GDE microgels after preparing their corresponding Ca(II), Mg(II), and Ba(II) complexes were investigated. Accordingly, NaOH treated bPEI-GDE and lPEI-GDE microgels were studied due to their high CO_2 adsorption capacity and their potential to interact with more metal ions due to being deprotonated. In Figure 4a, the CO_2 adsorption capacity of the NaOH treated bPEI-GDE microgel and the Ca(II), Mg(II) and Ba(II) complexes of these microgels are compared. As can be clearly seen, the formation of metal ion complexes is affected by the CO_2 adsorption capacity of the NaOH treated bPEI-GDE microgels, increased their adsorption capacity. The adsorbed amount of CO_2 by NaOH treated bPEI-GDE-Ca(II), -Mg(II), and Ba(II) microgel complexes were determined as 7.45 ± 0.51, 5.17 ± 0.36, and 9.48 ± 0.69 cm^3 CO_2/g, respectively, which are clearly higher than NaOH treated bPEI-GDE microgels.

Moreover, the CO_2 adsorption capacities of metal ion complexes of NaOH treated lPEI-GDE microgels were also compared in Figure 4b. The increasing on adsorption capacity of NaOH treated lPEI-GDE microgels at 900 mm Hg and 25°C after preparation -Ca(II), -Mg(II), and -Ba(II) complexes were seen. The CO_2 adsorption amount for NaOH treated lPEI-GDE-Ca(II), -Mg(II), and Ba(II) microgel complexes were determined as 11.07 ± 1.07, 9.55 ± 0.97, and 14.51 ± 1.09 cm^3 CO_2/g, respectively. From Figure 4a,b, it can be clearly said that the adsorption amount of metal ion complexes of lPEI-GDE microgels are higher than bPEI-GDE microgels. However, for better comparison the adsorbed amount of CO_2 (mmol/g) by PEI-based microgel complexes were summarized in Table 2.

It was clearly seen that, the higher CO_2 adsorption amounts were calculated for Ba(II) complexes of NaOH treated both bPEI-GDE, and lPEI-GDE microgels among the other metal ion complexes with 0.46 ± 0.03 and 0.70 ± 0.05 mmol CO_2/g, respectively, which are almost 13-fold, and 7.5-fold higher than their form that do not contain metal ions. On the other hand, the NaOH treated bPEI-GDE-Ca(II), and -Mg(II) complexes also exhibited almost 10 and 7-fold higher CO_2 adsorption capacity then bare NaOH treated bPEI-GDE microgels. The prepared NaOH treated lPEI-GDE-Ca(II), and -Mg(II) complexes also showed almost 6- and 5-fold higher CO_2 adsorption than bare form, respectively. Similar tendency for metal ion complexes of NaOH treated both bPEI-GDE, and lPEI-GDE microgels such as higher CO_2 adsorption capacities with -Ba(II) > Ca(II) > Mg(II) ion complexes, respectively. This trend is compatible with reported studies in literature,[90,92] and can be explained by the fact that Ba(II) has a larger ionic radius than Ca(II) and Mg(II). The enhanced CO_2 adsorption was observed for metal ion doped PEI based microgels and this can be explained by the decrease in steric hindrance which is a consequence of the higher radii of the metal ions and the stronger attraction exerted by the heavier metal ions.[90] Because (i) greater ionic radii lengthen the connection between adjacent oxygen atoms, exposing the positive charge of metals sufficiently to interact with CO_2, and (ii) bigger elements have stronger dispersion interactions with CO_2, there is an increase in the quantity of CO_2 adsorption with ionic radii.[92] On the other hand, the comparison of calculated increases on CO_2 adsorption capacities of NaOH treated bPEI-GDE, and lPEI-GDE microgels after preparation metal ion complexes, higher increases were observed for bPEI-GDE microgel complexes for each metal ion complexes. It can be explained with the possible higher metal ion adsorption of bPEI-GDE microgels than lPEI-GDE microgels due to higher amount of primary amine groups on structure.

3.3 | CO_2 adsorption capacities of PEI-based cryogels

As a result of the promising results of bPEI and lPEI-based microgels cross-linked with GDE for CO_2

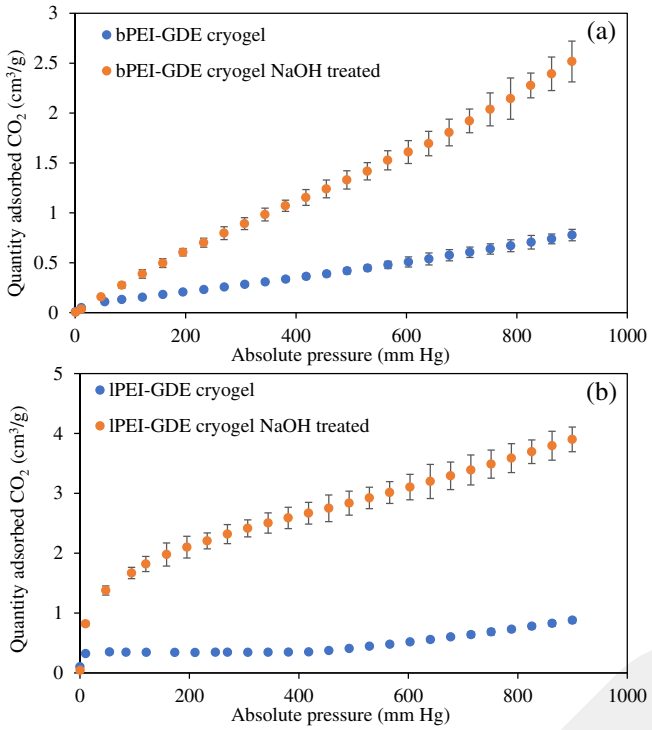

FIGURE 5 The comparison of CO_2 adsorption ability of (a) bPEI, and (b) lPEI cryogels with their corresponding NaOH treated forms. [Color figure can be viewed at wileyonlinelibrary.com]

TABLE 3 The comparison of CO_2 adsorption capacities of GDE crosslinked PEI based cryogels done at 25°C temperature and 900 mmHg pressures.

Materials (cryogels)	Quantity adsorbed CO_2 (mmol/g)
bPEI-GDE	0.038
bPEI-GDE NaOH	0.122
lPEI-GDE	0.042
lPEI-GDE NaOH	0.189

adsorption studies, the potential CO_2 adsorption capacities of bPEI and lPEI cryogels prepared by cross-linking with GDE,[68,72] previously reported by our group, were also examined. In Figure 5a, the CO_2 adsorption capacities of bPEI-GDE cryogel and NaOH treated bPEI-GDE cryogels were compared, and 0.78 ± 0.06, and 2.52 ± 0.20 cm^3 CO_2/g adsorption were observed, respectively.

On the other hand, from Figure 5b, the CO_2 adsorption capacities of lPEI-GDE, and NaOH treated lPEI-GDE cryogels were determined as 0.88 ± 0.04 and 3.90 ± 0.20 cm^3 CO_2/g, respectively. Moreover, the calculated adsorbed mmol CO_2 amounts by PEI based cryogels were compared in Table 3.

From the result, the lPEI-GDE-based cryogels adsorbed higher amounts of CO_2 than bPEI-GDE- based cryogels. The bPEI-GDE cryogels adsorbed 0.038 ± 0.003 mmol CO_2/g, whereas lPEI-GGDE cryogels adsorbed 0.042 ± 0.002 mmol CO_2/g. On the other hand, the NaOH treatments of bPEI-GDE, and lPEI-GDE cryogels provide almost 3- and 5-fold higher CO_2 adsorption amounts with 0.122 ± 0.01 and 0.188 ± 0.01 mmol CO_2/g, respectively, according to their untreated forms. In addition, all PEI-based cryogels showed higher CO_2 adsorption capacities than their corresponding PEI-based microgels. The interconnected super porous structure of the prepared bPEI-GDE and lPEI-GDE cryogels was associated with having better adsorption capacities than PEI-based microgels under the same conditions.

3.4 | The reusability of GDE crosslinked bPEI and lPEI microgels, and cryogels on CO_2 adsorption studies

The biggest possibility for the adsorbents used in research on CO_2 removal to have a high potential for use in industrial applications is that they are economically suitable.[6,8,16–18,93] There are two important ways to achieve this: (1) the material prepared as an adsorbent is affordable, (2) the cost is reduced by the good reusability of the prepared adsorbent. For this reason, the reuse potential of bPEI-GDE and lPEI-GDE microgels and cryogels treated with NaOH used in this study was investigated and the relevant graphs are given in Figure 6. In reuse studies, for the first time, adsorbents that adsorbed CO_2 were kept at 120°C for 6 h to desorb the CO_2 they adsorbed, and after the degas process, their CO_2 adsorption capacities were examined again. In Figure 6a, the amount of CO_2 adsorbed by NaOH treated bPEI-GDE and lPEI-GDE microgels after repeated reuse is compared in millimole per gram. Accordingly, the adsorbed amount of CO_2 by both NaOH treated bPEI-GDE, and lPEI-GDE microgels decreased after 10 consecutive uses. The adsorbed amount of CO_2 by NaOH treated bPEI-GDE microgels decreased from the 0.036 ± 0.002 mmol CO_2/g to 0.022 ± 0.002 mmol CO_2/g, whereas decreased from 0.094 ± 0.006 mol CO_2/g to 0.046 ± 0.004 mmol CO_2/g for NaOH treated lPEI-GDE microgels after 10 repetitive usages. The decrease on activities% of both NaOH treated bPEI-GDE, and lPEI-GDE microgels were also compared in Figure 6b. It was observed that, the NaOH treated bPEI-GDE microgels maintained >80% activity after five consecutive usages and provide 60.5 ± 8.5% activity after 10th usage. On the other hand, NaOH treated lPEI-GDE microgels preserved >80% activity after three usages, however almost 50% activity loss was observed after 10 repetitive usages.

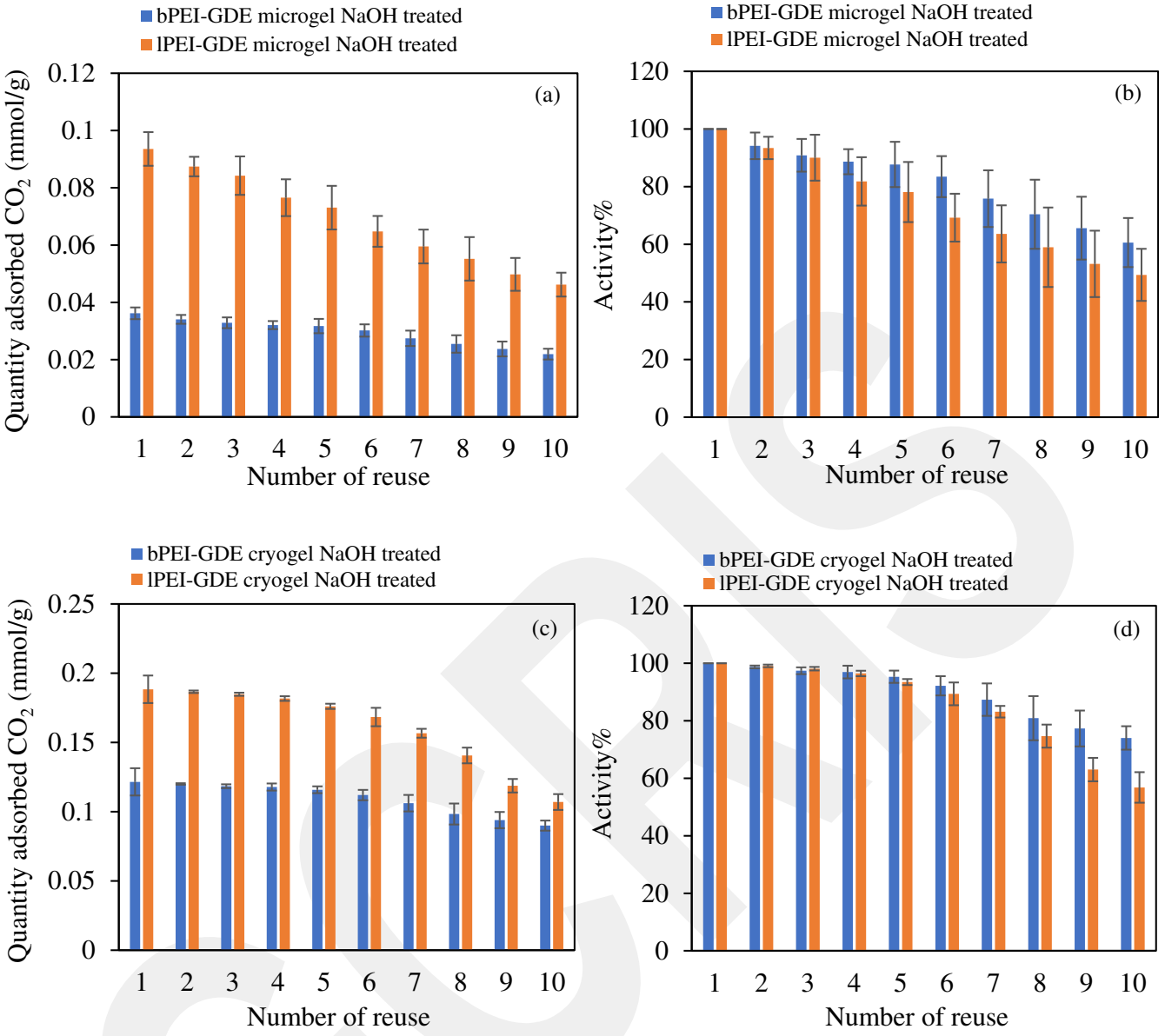

FIGURE 6 The changing on (a) CO_2 adsorption capacity, and (b) %activity of PEI-GDE microgels, and the changing on (c) CO_2 adsorption capacity, and (d) %activity of PEI-GDE cryogels. [Color figure can be viewed at wileyonlinelibrary.com]

The reusability of NaOH treated bPEI-GDE, and lPEI-GDE cryogels were also compared in Figure 6c,d. In Figure 6c, the changing on adsorbed amount of CO_2 by NaOH treated bPEI-GDE, and lPEI-GDE microgels in consecutive usages were compared. Here, the adsorbed amount of absorbed CO_2 by NaOH treated bPEI-GDE cryogels were calculated as 0.121 ± 0.01 mmol CO_2/g for first usage and decreased to 0.090 ± 0.004 mmol CO_2/g after 10 repetitive usages. Similarly, the adsorbed amount of CO_2 by NaOH treated lPEI-GDE cryogels decreased from 0.188 ± 0.01 mmol CO_2/g to 0.107 ± 0.006 mmol CO_2/g after 10 times usages. The activity% of adsorbents were also compared in Figure 6d. The NaOH treated bPEI-GDE cryogels exhibited almost 90% activity for seven consecutive usages and preserved its after 10th usage. However, the NaOH treated lPEI-GDE cryogels maintained almost 90% activity after 6 consecutive usage and exhibited 56.8 ± 5.3% activity even after 10 repetitive usages.

In overall, bPEI-GDE based microgels and cryogels showed better reusability properties with 60.5 ± 8.5 and 74.0 ± 4.1% activity, the lPEI-GDE based microgels and cryogels after 10 consecutive usages. On the other hand, both bPEI-GDE and lPEI-GDE cryogels exhibited better reusability than bPEI-GDE and lPEI-GDE microgels with higher activity% values. It was also reported in literature that, epoxy modification of PEI provide better

desorption properties on CO_2 adsorption studies for better reusability.[94]

3.5 | Overall, and comparison with related materials reported in literature

In the present study, the higher CO_2 adsorption capacities were observed for NaOH treated lPEI-based microgels and cryogels according to their bPEI forms with 0.094 ± 0.006 and 0.188 ± 0.01 mmol CO_2/g, respectively. On the other hand, the prepared NaOH treated bPEI-GDE-Ba(II), and lPEI-GDE-Ba(II) microgel complexes exhibited 13- and 7.5-fold higher adsorption capacities than their bare forms. The results obtained for bPEI-GDE, and lPEI-GDE based microgels and cryogels, which showed the best CO_2 adsorption capacity throughout the study, were compared with the results obtained for similar materials in the literature. However, there are limited numbers of studies where crosslinked PEI-based materials are used for CO_2 adsorption.[95–100] Accordingly, it has been reported in the literature that microgels crosslinked with 150% DVS using lPEI chains with different molecular weights such as 2.5, 5, and 10 K adsorb approximately 1–4 mmol CO_2/g under 25°C and 1 bar pressure conditions.[95] In another study, the CO_2 adsorption capacity of bPEI78 and bPEI196 scaffold, prepared by cross-linking bPEI with a molecular weight of 750 K with poly(ethylene glycol) diglycidyl ether (PEGDGE) at reaction temperatures of −78 and 196°C, was found to be 2.1 and 2.3 mmol CO_2/g, respectively.[96] In the same study, it was also shown that bPEI78 scaffold lost approximately 70% of its CO_2 adsorption capacity when used 10 times in a row.[96] In the study conducted by Hamdy et al., bPEI (25 K molecular weight) was crosslinked with 2,4,6-Tris-[4-(bromomethyl-3-fluoro)-phenyl]-1,3,5-triazine (4BMFPT) at different rates as 1:1, 3:1, and 5:1.[97] It has been reported that porous bPEI-based adsorbents prepared by cross-linking at different rates as 1:1, 3:1 and 5:1 have adsorption capacities of 1.17, 1.44, and 1.28 mmol CO_2/g at 30°C and 1 atm conditions, respectively.[97] Xu et al., have focused on CO_2 adsorption properties of crosslinked PEI based structures.[98–100] The prepared bPEI (25 K molecular weight) based crosslinked beads adsorbed 60.2 mg CO_2/g at 2 bar.[100] Also, the named PEI-snow structure prepared by Xu et al., via crosslinking of bPEI (25 K molecular weight) with triglycidyl trimethylolpropane ether exhibited 50 mg CO_2/g adsorption capacity via direct air capture of CO_2 under air flow rate of 2000 mL/min.[98] Moreover, the higher CO_2 adsorption capacity for crosslinked PEI based structures so far were also reported by Xu et al., which is crosslinked bPEI with 1,3-butadiene diepoxide with 415 mg CO_2/g at 1.02–1.04 bar.[99]

Although there are many PEI-based adsorbents which are generally PEI-modified forms of materials with high surface areas such as carbon particles (CPs),[101–105] zeolitic imidazolate frameworks (ZIFs),[58,106–110] metal organic frameworks (MOFs),[60,111–115] silica based materials,[116–120] and so forth.[59,121–127] In brief, the modification of various materials with PEI improves their CO_2 adsorption capacities, and selectivity. Therefore, the prepared PEI based crosslinked microgels and cryogels are promising material for CO_2 capture.

4 | CONCLUSION

Firstly, the NaOH treated PEI based materials used in this study revealed an enhanced CO_2 adsorption capacity, and disclosed evidence that PEI based structures used in this study adsorbed CO_2 in accordance with zwitterion mechanism. In comparison of CO_2 adsorption capacities of NaOH treated DVS, PNC, and GDE crosslinked bPEI microgels, it was found that bPEI-GDE microgels exhibited better adsorption capacity with 0.036 ± 0.002 mmol CO_2/g at 900 mm Hg, 25°C. According to the zwitterion mechanism, probably, one amine (a Lewis base) assists in proton transfer or exchange while the second amine (a Bronsted base) acts as the nucleophile, targeting the carbon in CO_2.[128] In addition, it is normal for PEI microgels cross-linked with GDE to have a greater CO_2 adsorption capability given that surface hydroxyl groups can also aid in the proton transfer process.[77,129] Because the opened epoxy rings become hydroxyl groups in epoxy-amine reactions. On the other hand, NaOH treated lPEI-GDE microgels showed higher CO_2 adsorption capacity with 0.094 ± 0.006 mmol CO_2/g than NaOH treated bPEI-GDE microgels. The higher CO_2 adsorption capacity of lPEI-GDE based microgels than bPEI-GDE based microgels was explained with the oxidation rates of amine groups, which directly affect the CO_2 adsorption capacity. Also, the improvement on CO_2 adsorption capacities of GDE crosslinked bPEI and lPEI microgels with simple modification was also presented with at least 2-fold increase in CO_2 adsorption capacities. Moreover, the PEHA modification of lPEI-GDE microgels improved CO_2 adsorption capacity 7.5-fold after NaOH treatment due to increasing number of amine groups in structure. The Ca(II), Mg(II), and Ba(II) metal ion complexes of NaOH treated bPEI-GDE and lPEI-GDE microgels afforded higher CO_2 adsorption capacities in order of Mg(II) < Ca(II) < Ba(II) complexes. This can be explained with

a bigger ionic radius of Ba(II) ions than Ca(II), and Mg(II) ions. On the other hand, the interconnected super porous structure of bPEI-GDE and lPEI-GDE cryogels presented higher CO_2 adsorption capacities than their related microgel forms. Moreover, the reusability studies revealed that even though the higher amount of CO_2 adsorption occurred with lPEI-GDE based microgels and cryogels, better reusability properties were observed for bPEI-GDE based microgels and cryogels. In conclusion, the prepared crosslinked PEI based microgels and cryogels are viable materials in CO_2 adsorption studies due to their tunable surface properties, material properties, higher number of amine groups, and ample reusability with convenient custom designable size, structures and morphologies.

AUTHOR CONTRIBUTIONS

Sahin Demirci: Data curation (lead); formal analysis (lead); investigation (equal); methodology (equal); validation (equal); writing – original draft (lead). **Erk Inger:** Data curation (supporting); formal analysis (lead); investigation (supporting); validation (equal); writing – original draft (equal). **Venkat Bhethanabotla:** Funding acquisition (supporting); resources (equal); supervision (equal); writing – review and editing (equal). **Nurettin Sahiner:** Conceptualization (lead); formal analysis (equal); funding acquisition (equal); investigation (equal); methodology (lead); resources (equal); validation (equal); visualization (lead); writing – review and editing (lead).

ACKNOWLEDGMENTS

This research was supported by the Scientific and Technological Research Council of Turkey (TUBITAK-BİDEB-2219) Postdoctoral Research Program, 1059B192202793.

DATA AVAILABILITY STATEMENT

No new data are generated.

ORCID

Nurettin Sahiner https://orcid.org/0000-0003-0120-530X

REFERENCES

[1] C. B. Field, K. J. Mach, *Science* **2017**, *356*, 706.
[2] T. Terlouw, C. Bauer, L. Rosa, M. Mazzotti, *Energy Environ. Sci.* **2021**, *14*, 1701.
[3] C. Pozo, Á. Galán-Martín, D. M. Reiner, N. Mac Dowell, G. Guillén-Gosálbez, *Nat. Clim. Chang.* **2020**, *10*, 640.
[4] E. Kriegler, O. Edenhofer, L. Reuster, G. Luderer, D. Klein, *Clim. Change* **2013**, *118*, 45.
[5] T. M. Gür, *Prog. Energy Combust. Sci.* **2022**, *89*, 100965.
[6] W. Gao, S. Liang, R. Wang, Q. Jiang, Y. Zhang, Q. Zheng, B. Xie, C. Y. Toe, X. Zhu, J. Wang, L. Huang, Y. Gao, Z. Wang, C. Jo, Q. Wang, L. Wang, Y. Liu, B. Louis, J. Scott, A.-C. Roger, R. Amal, H. He, S.-E. Park, *Chem. Soc. Rev.* **2020**, *49*, 8584.
[7] C. L. Fyson, S. Baur, M. Gidden, C.-F. Schleussner, *Nat. Clim. Chang.* **2020**, *10*, 836.
[8] A. I. Osman, M. Hefny, M. I. A. Abdel Maksoud, A. M. Elgarahy, D. W. Rooney, *Environ. Chem. Lett.* **2021**, *19*, 797.
[9] M. Zeynalian, A. H. Hajialirezaei, A. R. Razmi, M. Torabi, *Appl. Therm. Eng.* **2020**, *178*, 115593.
[10] S. Fuss, J. G. Canadell, G. P. Peters, M. Tavoni, R. M. Andrew, P. Ciais, R. B. Jackson, C. D. Jones, F. Kraxner, N. Nakicenovic, C. Le Quéré, M. R. Raupach, A. Sharifi, P. Smith, Y. Yamagata, *Nat. Clim. Chang.* **2014**, *4*, 850.
[11] J. Rogelj, D. Shindell, K. Jiang, S. Fifita, P. Forster, V. Ginzburg, C. Handa, K. Haroon, S. Kobayashi, E. Kriegler, L. Mundaca, R. Séférian, V. Vilariño, Mitigation Pathways Compatible with 1.5°C in the Context of Sustainable Development, Cambridge University Press, Cambridge, UK/ New York, NY, USA 2018, pp. 93–174, https://doi.org/10.1017/9781009157940.004
[12] K. Anderson, H. J. Buck, L. Fuhr, O. Geden, G. P. Peters, E. Tamme, *Nat. Rev. Earth Environ.* **2023**, *4*, 808.
[13] P. Smith, S. J. Davis, F. Creutzig, S. Fuss, J. Minx, B. Gabrielle, E. Kato, R. B. Jackson, A. Cowie, E. Kriegler, D. P. van Vuuren, J. Rogelj, P. Ciais, J. Milne, J. G. Canadell, D. McCollum, G. Peters, R. Andrew, V. Krey, G. Shrestha, P. Friedlingstein, T. Gasser, A. Grübler, W. K. Heidug, M. Jonas, C. D. Jones, F. Kraxner, E. Littleton, J. Lowe, J. R. Moreira, N. Nakicenovic, M. Obersteiner, A. Patwardhan, M. Rogner, E. Rubin, A. Sharifi, A. Torvanger, Y. Yamagata, J. Edmonds, C. Yongsung, *Nat. Clim. Chang.* **2016**, *6*, 42.
[14] A. J. Sykes, M. Macleod, V. Eory, R. M. Rees, F. Payen, V. Myrgiotis, M. Williams, S. Sohi, J. Hillier, D. Moran, D. A. C. Manning, P. Goglio, M. Seghetta, A. Williams, J. Harris, M. Dondini, J. Walton, J. House, P. Smith, *Glob. Chang. Biol.* **2020**, *26*, 1085.
[15] M. Honegger, W. Burns, D. R. Morrow, *Rev. Eur. Comp. Int. Environ. Law* **2021**, *30*, 327.
[16] S. Davoodi, M. Al-Shargabi, D. A. Wood, V. S. Rukavishnikov, K. M. Minaev, *Gas Sci. Eng.* **2023**, *117*, 205070.
[17] T. Wilberforce, A. G. Olabi, E. T. Sayed, K. Elsaid, M. A. Abdelkareem, *Sci. Total Environ.* **2021**, *761*, 143203.
[18] A. H. Alami, A. Abu Hawili, M. Tawalbeh, R. Hasan, L. Al Mahmoud, S. Chibib, A. Mahmood, K. Aokal, P. Rattanapanya, *Sci. Total Environ.* **2020**, *717*, 137221.
[19] D. M. D'Alessandro, B. Smit, J. R. Long, *Angew. Chemie Int. Ed.* **2010**, *49*, 6058.
[20] F. Hussin, M. K. Aroua, *J. Cleaner Prod.* **2020**, *253*, 119707.
[21] J. C. M. Pires, F. G. Martins, M. C. M. Alvim-Ferraz, M. Simões, *Chem. Eng. Res. Des.* **2011**, *89*, 1446.
[22] S. I. Eyitayo, C. J. Okere, A. Hussain, T. Gamadi, M. C. Watson, *J. Environ. Manage.* **2024**, *351*, 119713.
[23] C. G. Piscopo, S. Loebbecke, *Chempluschem* **2020**, *85*, 538.
[24] B. P. Spigarelli, S. K. Kawatra, *J. CO2 Util.* **2013**, *1*, 69.
[25] D. Bilanovic, A. Andargatchew, T. Kroeger, G. Shelef, *Energy Convers. Manage.* **2009**, *50*, 262.

[26] K. Skjånes, P. Lindblad, J. Muller, *Biomol. Eng.* **2007**, *24*, 405.
[27] C. Stewart, M.-A. Hessami, *Energy Convers. Manage.* **2005**, *46*, 403.
[28] R. S. Haszeldine, *Science* **2009**, *325*, 1647.
[29] E. Nessi, A. I. Papadopoulos, P. Kazepidis, A. Polychroniadis, G. Ntourou, S. Voutetakis, P. Seferlis, *J. Environ. Manage.* **2022**, *317*, 115489.
[30] S. C. Galusnyak, L. Petrescu, C.-C. Cormos, *J. Environ. Manage.* **2022**, *320*, 115908.
[31] F. Meng, Y. Meng, T. Ju, S. Han, L. Lin, J. Jiang, *Renew. Sustain. Energy Rev.* **2022**, *168*, 112902.
[32] F. Shakerian, K.-H. Kim, J. E. Szulejko, J.-W. Park, *Appl. Energy* **2015**, *148*, 10.
[33] E. E. Ünveren, B. Ö. Monkul, Ş. Sarıoğlan, N. Karademir, E. Alper, *Petroleum* **2017**, *3*, 37.
[34] G. T. Rochelle, *Science* **2009**, *325*, 1652.
[35] Q. Wang, J. Luo, Z. Zhong, A. Borgna, *Energy Environ. Sci.* **2011**, *4*, 42.
[36] L. Nie, Y. Mu, J. Jin, J. Chen, J. Mi, *Chinese J. Chem. Eng.* **2018**, *26*, 2303.
[37] A. Kaithwas, M. Prasad, A. Kulshreshtha, S. Verma, *Chem. Eng. Res. Des.* **2012**, *90*, 1632.
[38] M. Pardakhti, T. Jafari, Z. Tobin, B. Dutta, E. Moharreri, N. S. Shemshaki, S. Suib, R. Srivastava, *ACS Appl. Mater. Interfaces* **2019**, *11*, 34533.
[39] S. J. J. Titinchi, M. Piet, H. S. Abbo, O. Bolland, W. Schwieger, *Energy Procedia* **2014**, *63*, 8153.
[40] M. Minelli, V. Medri, E. Papa, F. Miccio, E. Landi, F. Doghieri, *Chem. Eng. Sci.* **2016**, *148*, 267.
[41] M. Younas, M. Sohail, L. K. Leong, M. J. Bashir, S. Sumathi, *Int. J. Environ. Sci. Technol.* **1839**, *2016*, 13.
[42] L. Lin, Y. Meng, T. Ju, S. Han, F. Meng, J. Li, Y. Du, M. Song, T. Lan, J. Jiang, *J. Environ. Manage.* **2023**, *325*, 116438.
[43] P. Zhao, G. Zhang, H. Yan, Y. Zhao, *Chinese J. Chem. Eng.* **2021**, *35*, 17.
[44] A. Samanta, A. Zhao, G. K. H. Shimizu, P. Sarkar, R. Gupta, *Ind. Eng. Chem. Res.* **2012**, *51*, 1438.
[45] M. Olivares-Marín, M. M. Maroto-Valer, *Greenh. Gases Sci. Technol.* **2012**, *2*, 20.
[46] R. Balasubramanian, S. Chowdhury, *J. Mater. Chem. A* **2015**, *3*, 21968.
[47] S.-Y. Lee, S.-J. Park, *J. Ind. Eng. Chem.* **2015**, *23*, 1.
[48] B. Dziejarski, J. Serafin, K. Andersson, R. Krzyżyńska, *Mater. Today Sustain.* **2023**, *24*, 100483.
[49] H. F. Hasan, F. T. Al-Sudani, T. M. Albayati, I. K. Salih, H. N. Hharah, H. S. Majdi, N. M. Cata Saady, S. Zendehboudi, A. Amari, S. A. Gheni, *Process Saf. Environ. Prot.* **2024**, *182*, 975.
[50] J. Wang, L. Huang, R. Yang, Z. Zhang, J. Wu, Y. Gao, Q. Wang, D. O'Hare, Z. Zhong, *Energy Environ. Sci.* **2014**, *7*, 3478.
[51] Y. Wang, L. Liu, C. Ren, J. Ma, B. Shen, P. Zhao, Z. Zhang, *J. Environ. Manage.* **2024**, *349*, 119540.
[52] A. A. Al-Absi, A. Domin, M. Mohamedali, A. M. Benneker, N. Mahinpey, *Fuel* **2023**, *333*, 126401.
[53] A. M. Varghese, G. N. Karanikolos, *Int. J. Greenhouse Gas Control* **2020**, *96*, 103005.
[54] W. Li, S. Choi, J. H. Drese, M. Hornbostel, G. Krishnan, P. M. Eisenberger, C. W. Jones, *ChemSusChem* **2010**, *3*, 899.
[55] G. Qi, L. Fu, E. P. Giannelis, *Nat. Commun.* **2014**, *5*, 5796.
[56] A. Sayari, Y. Belmabkhout, E. Da'na, *Langmuir* **2012**, *28*, 4241.
[57] A. Heydari-Gorji, Y. Belmabkhout, A. Sayari, *Microporous Mesoporous Mater.* **2011**, *145*, 146.
[58] J. Cheng, N. Liu, L. Hu, Y. Li, Y. Wang, J. Zhou, *Chem. Eng. J.* **2019**, *364*, 530.
[59] W. Wang, F. Liu, Q. Zhang, G. Yu, S. Deng, *Chem. Eng. J.* **2020**, *399*, 125734.
[60] C. Choi, R. L. Kadam, S. Gaikwad, K.-S. Hwang, S. Han, *Microporous Mesoporous Mater.* **2020**, *296*, 110006.
[61] K. Başaran, B. U. Topçubaşı, T. Davran-Candan, *J. CO2 Util.* **2021**, *47*, 101492.
[62] M. Caplow, *J. Am. Chem. Soc.* **1968**, *90*, 6795.
[63] N. Sahiner, *Colloids Surf. A* **2013**, *433*, 212.
[64] S. Demirci, N. Sahiner, *Water, Air, Soil Pollut.* **2015**, *226*, 226.
[65] N. Sahiner, S. Demirci, *Eur. Polym. J.* **2016**, *76*, 156.
[66] S. Demirci, M. Yildiz, N. Sahiner, *J. Environ. Chem. Eng.* **2024**, *12*, 112066.
[67] S. Bagdat, F. Tokay, S. Demirci, S. Yilmaz, N. Sahiner, *J. Environ. Manage.* **2023**, *329*, 117002.
[68] M. Sahiner, A. S. Yilmaz, S. Demirci, N. Sahiner, *Biomedicines* **2023**, *11*, 706.
[69] S. Soradech, A. C. Williams, V. V. Khutoryanskiy, *Macromolecules* **2022**, *55*, 9537.
[70] N. Sahiner, S. Demirci, M. Sahiner, H. Al-Lohedan, *Appl. Surf. Sci.* **2015**, *354*, 380.
[71] S. Demirci, S. S. Suner, S. Yilmaz, S. Bagdat, F. Tokay, N. Sahiner, *Appl. Clay Sci.* **2024**, *249*, 107265.
[72] S. Kubilay, S. Demirci, M. Can, N. Aktas, N. Sahiner, *J. Environ. Chem. Eng.* **2021**, *9*, 104799.
[73] S. A. Didas, A. R. Kulkarni, D. S. Sholl, C. W. Jones, *ChemSusChem* **2012**, *5*, 2058.
[74] T. L. Donaldson, Y. N. Nguyen, *Ind. Eng. Chem. Fundam.* **1980**, *19*, 260.
[75] T. S. Nguyen, N. A. Dogan, H. Lim, C. T. Yavuz, *Acc. Chem. Res.* **2023**, *56*, 2642.
[76] Y. G. Ko, S. S. Shin, U. S. Choi, *J. Colloid Interface Sci.* **2011**, *361*, 594.
[77] K. Li, J. D. Kress, D. S. Mebane, *J. Phys. Chem. C* **2016**, *120*, 23683.
[78] A. Ahmadalinezhad, A. Sayari, *Phys. Chem. Chem. Phys.* **2014**, *16*, 1529.
[79] K. Min, W. Choi, C. Kim, M. Choi, *Nat. Commun.* **2018**, *9*, 9.
[80] H. J. Park, M. P. Suh, *Chem. Sci.* **2013**, *4*, 685.
[81] P. D. Wakchaure, B. Ganguly, *ACS Omega* **2020**, *5*, 31146.
[82] R. Chang, S. Kim, S. Lee, S. Choi, M. Kim, Y. Park, *Front. Energy Res.* **2017**, *5*, 5.
[83] A. Kuang, M. Kuang, H. Yuan, G. Wang, H. Chen, X. Yang, *Appl. Surf. Sci.* **2017**, *410*, 505.
[84] J. Tapiador, E. García-Rojas, P. López-Patón, G. Calleja, G. Orcajo, C. Martos, P. Leo, *J. Environ. Chem. Eng.* **2023**, *11*, 109497.
[85] X. Liu, L. Sun, W.-Q. Deng, *J. Phys. Chem. C* **2018**, *122*, 8306.
[86] H. Zhao, L. Shi, Z. Zhang, X. Luo, L. Zhang, Q. Shen, S. Li, H. Zhang, N. Sun, W. Wei, Y. Sun, *ACS Appl. Mater. Interfaces* **2018**, *10*, 3495.
[87] Y. Liu, Z. Meng, X. Guo, G. Xu, D. Rao, Y. Wang, K. Deng, R. Lu, *Phys. Chem. Chem. Phys.* **2017**, *19*, 28323.

[88] L. Zhou, Z. Niu, X. Jin, L. Tang, L. Zhu, *ChemistrySelect* **2018**, *3*, 12865.
[89] R. Belgamwar, A. Maity, T. Das, S. Chakraborty, C. P. Vinod, V. Polshettiwar, *Chem. Sci.* **2021**, *12*, 4825.
[90] J. Borycz, D. Tiana, E. Haldoupis, J. C. Sung, O. K. Farha, J. I. Siepmann, L. Gagliardi, *J. Phys. Chem. C* **2016**, *120*, 12819.
[91] T. Alghamdi, K. S. Baamran, M. U. Okoronkwo, A. A. Rownaghi, F. Rezaei, *Energy Fuels* **2021**, *35*, 4258.
[92] S.-T. Yang, J. Kim, W.-S. Ahn, *Microporous Mesoporous Mater.* **2010**, *135*, 90.
[93] Z. Zhang, S.-Y. Pan, H. Li, J. Cai, A. G. Olabi, E. J. Anthony, V. Manovic, *Renew. Sustain. Energy Rev.* **2020**, *125*, 109799.
[94] W. Choi, K. Min, C. Kim, Y. S. Ko, J. W. Jeon, H. Seo, Y.-K. Park, M. Choi, *Nat. Commun.* **2016**, *7*, 12640.
[95] M. E. Payne, Y. Lou, X. Zhang, N. Sahiner, N. R. Sandoval, D. F. Shantz, S. M. Grayson, *ACS Appl. Polym. Mater.* **2020**, *2*, 826.
[96] P. Narayanan, R. P. Lively, C. W. Jones, *Energy Fuels* **2023**, *37*, 5257.
[97] L. B. Hamdy, A. Gougsa, W. Y. Chow, J. E. Russell, E. García-Díez, V. Kulakova, S. Garcia, A. R. Barron, M. Taddei, E. Andreoli, *Mater. Adv.* **2022**, *3*, 3174.
[98] X. Xu, M. B. Myers, F. G. Versteeg, B. Pejcic, C. Heath, C. D. Wood, *Chem. Commun.* **2020**, *56*, 7151.
[99] X. Xu, B. Pejcic, C. Heath, M. B. Myers, C. Doherty, Y. Gozukara, C. D. Wood, *ACS Appl. Mater. Interfaces* **2019**, *11*, 26770.
[100] X. Xu, B. Pejcic, C. Heath, C. D. Wood, *J. Mater. Chem. A* **2018**, *6*, 21468.
[101] Q. Chen, S. Wang, K. R. Rout, D. Chen, *Catal. Today* **2021**, *369*, 69.
[102] Y. He, Y. Xia, J. Zhao, Y. Song, L. Yi, L. Zhao, *Appl. Phys. A: Mater. Sci. Process.* **2019**, *125*, 160.
[103] S.-H. Chai, Z.-M. Liu, K. Huang, S. Tan, S. Dai, *Ind. Eng. Chem. Res.* **2016**, *55*, 7355.
[104] Z. Tang, Z. Han, G. Yang, J. Yang, *Appl. Surf. Sci.* **2013**, *277*, 47.
[105] Y. Zhao, Y. Zhu, T. Zhu, G. Lin, M. Shao, W. Hong, S. Hou, *Ind. Eng. Chem. Res.* **2019**, *58*, 15506.
[106] C. Jiao, Z. Li, X. Li, M. Wu, H. Jiang, *Sep. Purif. Technol.* **2021**, *259*, 118190.
[107] X. Li, D. Wang, H. Ning, Y. Xin, Z. He, F. Su, Y. Wang, J. Zhang, H. Wang, L. Qian, Y. Zheng, D. Yao, M. Li, *Sep. Purif. Technol.* **2021**, *276*, 119305.
[108] F. Yang, T. Ge, X. Zhu, J. Wu, R. Wang, *Sep. Purif. Technol.* **2022**, *287*, 120535.
[109] Z. Hu, H. Zhang, X.-F. Zhang, M. Jia, J. Yao, *J. Memb. Sci.* **2022**, *662*, 120996.
[110] M. Usman, M. Y. Khan, T. Anjum, A. L. Khan, B. Hoque, A. Helal, A. S. Hakeem, B. A. Al-Maythalony, *Membranes* **2022**, *12*, 1055.
[111] Y. Lin, Q. Yan, C. Kong, L. Chen, *Sci. Rep.* **2013**, *3*, 14.
[112] S. Mutyala, M. Jonnalagadda, H. Mitta, R. Gundeboyina, *Chem. Eng. Res. Des.* **2019**, *143*, 241.
[113] J. Zhu, L. Wu, Z. Bu, S. Jie, B.-G. Li, *Ind. Eng. Chem. Res.* **2019**, *58*, 4257.
[114] S. Xian, Y. Wu, J. Wu, X. Wang, J. Xiao, *Ind. Eng. Chem. Res.* **2015**, *54*, 11151.
[115] J. Zhu, L. Wu, Z. Bu, S. Jie, B.-G. Li, *ACS Omega* **2019**, *4*, 3188.
[116] S. Jeon, J. Min, S. H. Kim, K. B. Lee, *Chem. Eng. J.* **2020**, *398*, 125531.
[117] K. Wang, H. Shang, L. Li, X. Yan, Z. Yan, C. Liu, Q. Zha, *J. Nat. Gas Chem.* **2012**, *21*, 319.
[118] K. Li, J. Jiang, F. Yan, S. Tian, X. Chen, *Appl. Energy* **2014**, *136*, 750.
[119] C. Chen, H. Xu, Q. Jiang, Z. Lin, *Energy* **2021**, *214*, 119093.
[120] Z. Ghazali, N. Suhaili, M. N. A. Tahari, M. A. Yarmo, N. H. Hassan, R. Othaman, *J. Mater. Res. Technol.* **2020**, *9*, 3249.
[121] E. P. Dillon, C. A. Crouse, A. R. Barron, *ACS Nano* **2008**, *2*, 156.
[122] F. Liu, W. Fu, S. Chen, *J. Appl. Polym. Sci.* **2020**, *137*, 1.
[123] Y. Yu, J. Wang, Y. Wang, W. Pan, C. Liu, P. Liu, L. Liang, C. Xu, Y. Liu, *J. Ind. Eng. Chem.* **2020**, *83*, 20.
[124] O. Johnson, B. Joseph, J. N. Kuhn, *J. Ind. Eng. Chem.* **2021**, *103*, 255.
[125] S. Zeng, X. Liang, M. Zhao, Y. Ren, H. Ma, Z. Zhu, Y. Wang, S. Wang, J. Zhao, G. Yang, X. Wang, F. Pan, G. He, Z. Jiang, *J. Memb. Sci.* **2024**, *698*, 122590.
[126] J. Fujiki, K. Yogo, *Energy Fuels* **2014**, *28*, 6467.
[127] X. Wan, X. Lu, J. Liu, Y. Pan, H. Xiao, *Ind. Eng. Chem. Res.* **2019**, *58*, 4979.
[128] R. Ben Said, J. M. Kolle, K. Essalah, B. Tangour, A. Sayari, *ACS Omega* **2020**, *5*, 26125.
[129] M. Cho, J. Park, C. T. Yavuz, Y. Jung, *Phys. Chem. Chem. Phys.* **2018**, *20*, 12149.

SUPPORTING INFORMATION

Additional supporting information can be found online in the Supporting Information section at the end of this article.

How to cite this article: S. Demirci, E. Inger, V. Bhethanabotla, N. Sahiner, *J. Appl. Polym. Sci.* **2024**, *141*(44), e56180. https://doi.org/10.1002/app.56180